

Analytically Informed Inverse Kinematics Solution at Singularities

Andreas Müller

Abstract Near kinematic singularities of a serial manipulator, the inverse kinematics (IK) problem becomes ill-conditioned, which poses computational problems for the numerical solution. Computational methods to tackle this issue are based on various forms of a pseudoinverse (PI) solution to the velocity IK problem. The damped least squares (DLS) method provides a robust solution with controllable convergence rate. However, at singularities, it may not even be possible to solve the IK problem using any PI solution when certain end-effector motions are prescribed. To overcome this problem, an analytically informed inverse kinematics (AI-IK) method is proposed. The key step of the method is an explicit description of the tangent aspect of singular motions (the analytic part) to deduce a perturbation that yields a regular configuration. The latter serves as start configuration for the iterative solution (the numeric part). Numerical results are reported for a 7-DOF Kuka iiwa.

Key words: Inverse kinematics, singularities, pseudoinverse, damped pseudoinverse, Newton–Raphson method, higher-order analysis, kinematic tangent cone.

1 Introduction

The numerical solution of the inverse kinematics (IK) problem of serial robotic manipulators near singularities has been a topic for many years. The damped least squares (DLS) method was introduced [12] as a computationally efficient method that is robust against singularities. Its robustness comes at the expense that the convergence rate, and thus the tracking accuracy, depends on a damping parameter. Various strategies for adaptively selecting the damping factor were proposed [1, 2, 5, 9] that are all based on some measure of distance to a singularity. A problem, which has not been addressed adequately in the literature, is that the DLS method, as well as other methods relying on a pseudoinverse (PI), may get stuck when a robot that is in a singularity is commanded to execute instantaneous EE motions that are not in the image space of the manipulator Jacobian. One reference where this was addressed is [3], where an IK solution is introduced that takes into account the second order kinematics, i.e. the Hessian in addition to the Jacobian. In this paper, a method for

Andreas Müller
Johannes Kepler University, Linz, Austria, e-mail: a.mueller@jku.at

solving the IK problem at singularities is introduced that does not suffer from this lock-up phenomenon. The key element of the method is an initial regularization of the Jacobian by means of a perturbation that will lead to nearby a regular configuration. This perturbation is deduced from an analytic description of possible singular motions through the singularity. The so obtained regularized configuration is used as initial value of the IK problem that can be solved with an undamped pseudoinverse method. Numerical results are reported for a 7-DOF Kuka LBR iiwa.

2 The Inverse Kinematics Problem

Denote with \mathbb{V}^n the joint space of a serial robot. The forward kinematics map $f : \mathbb{V}^n \rightarrow W$ assigns to a joint coordinate vector $\mathbf{q} \in \mathbb{V}^n$ an end-effector (EE) pose $\mathbf{C} \in W$ in workspace. The latter is a subspace $W \subset SE(3)$ of dimension m , according to the task. It is assumed in the following that $m \leq n$. If $m < n$, the manipulator is *kinematically redundant*. The EE-velocity $\mathbf{V} \in \mathfrak{w}$ is determined by the joint velocity $\dot{\mathbf{q}} \in \mathbb{R}^n$ as $\mathbf{V} = \mathbf{J}(\mathbf{q}) \dot{\mathbf{q}}$, where \mathbf{J} is the *geometric Jacobian*. Let m be the maximal rank of the FK-Jacobian, and $r := \text{rank } \mathbf{J}(\mathbf{q})$. A configuration $\mathbf{q} \in \mathbb{V}^n$ where $r < m$ are *forward kinematics singularities* of the manipulator. Motions with $r < m$ are called *singular motions*.

The *geometric IK problem* is to compute a joint coordinate vector for given EE-pose, i.e. to solve $\mathbf{q} = f^{-1}(\mathbf{C})$. This problem has no unique solution, for non-redundant as well redundant robots. Closed form solutions are known for special cases only [4, 10]. The *velocity IK problem* is to compute the joint velocity $\dot{\mathbf{q}}$ for given EE velocity \mathbf{V} , at a given configuration \mathbf{q} . A solution is given in terms of the weighted pseudoinverse as $\dot{\mathbf{q}} = \mathbf{J}_M^+ \mathbf{V}$. Here the weight \mathbf{M} serves as a metric on \mathbb{V}^n to homogenize different units in \mathbf{q} . This solution gives rise to a solution of the geometric IK problem. Best known are the CLIK algorithms [11], which combine numerical integration of the velocity relation with a regulator feedback to avoid drift. It thus relies on the (pseudo)inverse solution. The velocity IK solution also gives rise to iterative solution with a Newton–Raphson method.

When approaching a singularity the Jacobian becomes ill-conditioned. Kinematically this implies that small EE motions lead to large joint motions. Mathematically, a solution can be obtained that produces these (undesirable) motions, e.g. using SVD. To alleviate the problem of large motions, in [9, 12] the IK problem is amended by adding an additional damping term (thus the robot kinematics is changed), which leads to the damped least squares (DLS) method (see Sect. 3).

While the DLS provides a robust solution (despite the need for tuning the damping parameter λ), it may not allow for solving the IK problem when the desired EE motion can instantaneous not be produced by joint motions. A simple example is the 3R regional robot in Fig. 1a), which is in a singularity \mathbf{q}_0 . At this singular configuration, the Jacobian and its pseudoinverse are

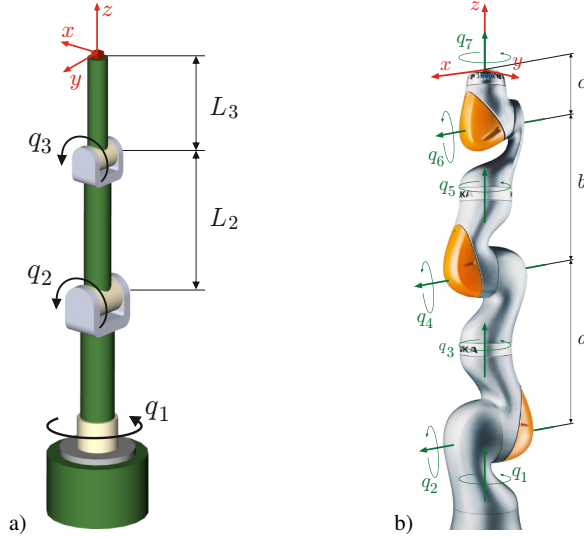


Fig. 1 a) 3R regional robot and b) 7-DOF Kuka iiwa 14 R820, both in a singular configuration.

$$\mathbf{J}(\mathbf{q}_0) = \begin{pmatrix} 0 & L_3 + L_2 & L_3 \\ 0 & 0 & 0 \\ 0 & 0 & 0 \end{pmatrix}, \quad \mathbf{J}^+(\mathbf{q}_0) = \begin{pmatrix} 0 & 0 & 0 \\ \frac{L_3 + L_2}{L_3^2 + (L_3 + L_2)^2} & 0 & 0 \\ \frac{L_1}{L_3^2 + (L_3 + L_2)^2} & 0 & 0 \end{pmatrix}. \quad (1)$$

Clearly, if the EE is commanded to move down in the y - z -plane, which corresponds to a prescribed velocity $\mathbf{V} = (0, v_y, v_z)$, the joint velocity computed from the IK is $\dot{\mathbf{q}} = \mathbf{0}$. Thus no solution to the geometric IK problem would be obtained until the EE is commanded to move also in x -direction. Note that the pseudoinverse (1) is the same when computed with an SVD or with the DLS method $\mathbf{J}_\lambda^+(\mathbf{q}_0)$ and setting $\lambda = 0$. The described phenomenon is not only problematic when the EE is commanded to move along instantaneously infeasible directions, but generally when solving the IK starting from a singularity.

A straightforward approach to tackle this issue is to perturb a singular configuration \mathbf{q}_0 by a vector $\boldsymbol{\varepsilon} \in \mathbb{R}^n$ of small joint increments, expecting $\mathbf{J}(\mathbf{q}_0 + \boldsymbol{\varepsilon})$ to be non-singular (but possibly ill-conditioned). Starting from $\mathbf{q}_0 + \boldsymbol{\varepsilon}$, the IK solution is computed. This approach relies on a proper choice of $\boldsymbol{\varepsilon}$. As the only purpose of $\boldsymbol{\varepsilon}$ is to get off the singularity, and since singularities form a set of measure zero, random values could be used for $\boldsymbol{\varepsilon}$. Random $\boldsymbol{\varepsilon}$ will unnecessarily deviate from the current \mathbf{q}_0 , however. Perhaps more critical is the fact that random values do not lead to a predetermined behavior of the solution. Instead, an informed choice is needed.

In this paper an IK solution method is proposed where $\boldsymbol{\varepsilon}$ delivers only the motions necessary to reach a nearby regular point. It employs results from the local analysis of singular motions, and is therefore called *Analytically Informed Inverse Kinematics Solution (AI-IK)* method.

3 Damped Least Squares (DLS) Solution

To avoid large joint motions near singularities, in [9, 12] IK solutions are sought such that $\|\mathbf{V} - \mathbf{J}(\mathbf{q})\dot{\mathbf{q}}\|^2 + \lambda^2 \|\dot{\mathbf{q}}\|^2$. This leads to the damped least squares (DLS) solution $\dot{\mathbf{q}} = \mathbf{J}_\lambda^+ \mathbf{V}$, with

$$\mathbf{J}_\lambda^+ = \mathbf{J}^T (\mathbf{J}\mathbf{J}^T + \lambda^2 \mathbf{I})^{-1} \quad (2)$$

where λ is a damping factor. The form (2) is equivalent to the original expression $\mathbf{J}_\lambda^+ = (\mathbf{J}^T \mathbf{J} + \lambda^2 \mathbf{I})^{-1} \mathbf{J}^T$. Written in this way, it is obvious that \mathbf{J}_λ^+ becomes the (non-weighted) right pseudoinverse when $\lambda = 0$. It will therefore be called the *damped pseudoinverse (DPI)*. This form is also numerically better conditioned.

The Jacobian is a $m \times n$ matrix of rank $r \leq \min(m, n)$. Using the singular value decomposition (SVD), the Jacobian is written as $\mathbf{J} = \mathbf{U}\mathbf{\Sigma}\mathbf{V}^T$, with $\mathbf{\Sigma} = \text{diag}(\sigma_1, \dots, \sigma_r, 0, \dots, 0)$, where σ_i are the non-zero singular values of \mathbf{J} . The left pseudoinverse can then be expressed as $\mathbf{J}^+ = \mathbf{V}\mathbf{\Sigma}^+\mathbf{U}^T$ with $\mathbf{\Sigma}^+ = \text{diag}(\frac{1}{\sigma_1}, \dots, \frac{1}{\sigma_r}, 0, \dots, 0)$. The DPI possesses the similar expression $\mathbf{J}_\lambda^+ = \mathbf{V}\mathbf{\Sigma}_\lambda^+\mathbf{U}^T$, with $\mathbf{\Sigma}_\lambda^+ = \text{diag}(\frac{\sigma_1}{\sigma_1^2 + \lambda^2}, \dots, \frac{\sigma_r}{\sigma_r^2 + \lambda^2}, 0, \dots, 0)$.

For $\lambda \rightarrow 0$, the DPI becomes the left pseudoinverse $\mathbf{J}_{\lambda=0}^+ = \mathbf{J}^+$. From this form it is clear that the damping parameter λ regularizes the solution. Even if \mathbf{J} is regular, i.e. $r = m$, near singularities, the smallest singular value σ_r becomes small, and the matrix to be inverted ill-conditioned. This is avoided with sufficiently large λ . On the other hand, large λ slow down the convergence of the iterative solution. Several methods for adaptation of the damping factor λ were proposed [1, 2, 5, 9].

In the expression for \mathbf{J} , the first r columns of $\mathbf{U}\mathbf{\Sigma}$ form a basis for the image space of \mathbf{J} , and the remaining columns (those multiplied with zero $\sigma_{r+1}, \dots, \sigma_m$) span the space of twists that cannot be generated. Thus, velocities $\mathbf{V} \in \ker \mathbf{\Sigma}_\lambda^+ \mathbf{U}^T$ always lead to $\dot{\mathbf{q}} = \mathbf{0}$. Any form of pseudoinverse method cannot solve the instantaneous IK problem when the commanded EE-velocity can instantaneously not be generated by the manipulator.

4 Iterative Solution of Inverse Kinematics

Throughout the rest of this paper, $W = SE(3)$ is assumed, for simplicity. Let $\mathbf{q} \in \mathbb{V}^n$ be the joint coordinate vector in the current pose, and $\mathbf{C}_d \in SE(3)$ the desired EE-pose. The 'difference' of the desired and the current EE pose (i.e. the transformation from desired to current configuration) is

$$\Delta \mathbf{C}(\mathbf{q}) = \mathbf{C}^{-1}(\mathbf{q}) \mathbf{C}_d. \quad (3)$$

Let $\mathbf{q}_d \in \mathbb{V}^n$ be a (unknown) joint coordinate vector corresponding to the desired \mathbf{C}_d . The IK problem is then to compute $\Delta \mathbf{q}_d$ such that $\mathbf{q}_d = \mathbf{q} + \Delta \mathbf{q}_d$. For small deviations, it is $\Delta \mathbf{C} - \mathbf{I} \in se(3)$, and the first-order approximation of (3) yields

$$\Delta \mathbf{q} = \mathbf{J}^+(\mathbf{q}) \Delta \mathbf{C}(\mathbf{q})^\vee \quad (4)$$

where $\mathbf{A}^\vee \in \mathbb{R}^6$ denotes the vector corresponding to $\mathbf{A} \in se(3)$. Here \mathbf{J}^+ is an appropriately chosen inverse, e.g. the DPI. The so obtained $\Delta \mathbf{q}$ will usually not solve the IK problem. Therefore, step (4) is repeated with \mathbf{q} replaced by $\mathbf{q} + \Delta \mathbf{q}$ until the error tracking satisfies $\|\Delta \mathbf{C} - \mathbf{I}\|_{\mathbf{M}} \leq \varepsilon$, where $\|\cdot\|_{\mathbf{M}}$ is a left-invariant metric on $SE(3)$. Notice that $\Delta \mathbf{C} - \mathbf{I} \approx \log \Delta \mathbf{C}$ is a first-order approximation of the logarithm on $SE(3)$, i.e. $\Delta \mathbf{C}(\mathbf{q}) = \exp(\Delta \mathbf{C} - \mathbf{I})$ holds true for small deviations. If the DPI is used in (4), this resembles the Levenberg-Marquardt method.

The solution (4) can be complemented by a null-space solution in case of redundant robots ($m < n$). The velocity command sent to the robot controller is $\Delta \mathbf{q}/T$, with T being the sampling time.

5 Analytically Informed Numerical IK Solution

5.1 The Analytical Part —Identifying Singular Motions

In the analytic step, directions of motion transversal to the singular motions are determined. This is pursued independently of the trajectory tracking, which implies that singularities are known before task execution.

Assumption 1 *The singular locus is either locally a manifold or it is the intersection of smooth manifolds (e.g. bifurcations), i.e. there are smooth singular motions.*

This assumption is by no means restrictive as it is very rare that the singular locus is not the intersection of lower-dimensional manifolds. Tangents to finite singular motions can be determined via higher-order local analysis [6, 7]. Denote with $L_m = \{\mathbf{q} \in \mathbb{V}^n | \text{rank } \mathbf{J}(\mathbf{q}) < m\}$ the variety of singular motions. At $\mathbf{q} \in L_m$ the kinematic tangent cone $C_{\mathbf{q}}^{\mathbf{K}} L_m \subset \mathbb{R}^n$ is the set of tangents to smooth finite singular motions through \mathbf{q} . The kinematic tangent cone is easily computed with a higher-order local analysis using the instantaneous joint screws (columns of \mathbf{J}). Closed form and recursive algorithms were reported [8]. With the above assumption, the tangent cone $C_{\mathbf{q}}^{\mathbf{K}} L_m = K_{\mathbf{q}}^{m(1)} \cup \dots \cup K_{\mathbf{q}}^{m(\bar{m})}$ is the union of \bar{m} vector spaces $K_{\mathbf{q}}^{m(i)}$, $i = 1, \dots, \bar{m}$ of dimensions less than n . Denote with $\mathbf{s}_1, \dots, \mathbf{s}_{\bar{s}} \in \mathbb{R}^n$ a set of \bar{s} vectors that form a basis on $K_{\mathbf{q}}^{m(1)} \cap \dots \cap K_{\mathbf{q}}^{m(\bar{m})}$, and introduce the matrix $\mathbf{S} = (\mathbf{s}_1, \dots, \mathbf{s}_{\bar{s}}) \in \mathbb{R}^n$.

5.2 The Numerical Part —Regularizing the Jacobian

The above discussion provides a means to solve the inverse kinematics at singularities. To this end, introduce the projector $\mathbf{N} = \mathbf{S}\mathbf{S}^T - \mathbf{I}$ to the orthogonal complement of \mathbf{S} . Let $\boldsymbol{\varepsilon} \in \mathbb{R}^n$ be an arbitrary vector. Its projection $\mathbf{x} = \mathbf{N}(\mathbf{q}) \boldsymbol{\varepsilon}$ is transversal to singular motions through \mathbf{q} , and \mathbf{x} represents tangents to motions away from the singular locus. For sufficiently large $\boldsymbol{\varepsilon}$, the prolonged Jacobian $\mathbf{J}(\mathbf{q}_0 + \mathbf{x})$ is regular (recall singularities form a lower-dimensional set in \mathbb{V}^n). The IK is solved with $\mathbf{J}(\mathbf{q}_0 + \mathbf{x})$ in (4), where \mathbf{x} is determined with a predefined vector of joint perturbations $\boldsymbol{\varepsilon}$. This method yields a motion (according to prescribed $\boldsymbol{\varepsilon}$) for leaving the

singularities. The conditioning of $\mathbf{J}(\mathbf{q}_0 + \mathbf{x})$ depends on the magnitude of $\boldsymbol{\varepsilon}$. If sufficiently large (e.g. in the order of the damping λ^2), $\mathbf{J}(\mathbf{q}_0 + \mathbf{x})$ is regular, and a non-regularized inverse is applicable.

In summary, the analytically informed inverse kinematics (AI-IK) method consists in iteratively solving the IK problem starting with the analytically regularized Jacobian $\mathbf{J}(\mathbf{q}_0 + \mathbf{x})$. In other words, the AI-IK method is the standard IK method where the first iteration step is replaced by the regularizing increment \mathbf{x} .

5.3 Analytic Calculation of the Prolonged Jacobian

The Jacobian at the perturbed configuration can be expressed as $\mathbf{J}(\mathbf{q}_0 + \mathbf{x}) = \mathbf{J}(\mathbf{q}_0) + d\mathbf{J}(\mathbf{q}_0, \mathbf{x}) + \frac{1}{2}d^2\mathbf{J}(\mathbf{q}_0, \mathbf{x}) + \dots$, where the k th-order differential $d^k\mathbf{J}(\mathbf{q}_0, \mathbf{x})$ is a k th-degree monomial in x_i . The order up to which this series must be written in order to obtain a regular Jacobian can be determined exactly for a given robot. Column i of $\mathbf{J} = (\mathbf{J}_1, \dots, \mathbf{J}_n)$ is the instantaneous screw coordinate vector \mathbf{J}_i of joint i expressed in EE-frame. Its first differential is given as $d\mathbf{J}_i(\mathbf{q}, \mathbf{x}) = \sum_{i < j \leq n} x_j [\mathbf{J}_i, \mathbf{J}_j]$, where $[\mathbf{J}_i, \mathbf{J}_j]$ is the Lie bracket of the two screws [8]. Thus $d\mathbf{J}(\mathbf{q}_0, \mathbf{x})$ involves the Lie brackets of all joint screws multiplied with x_i , and the image of $\mathbf{J}(\mathbf{q}_0) + d\mathbf{J}(\mathbf{q}_0, \mathbf{x})$ is contained in $\text{span}(\mathbf{J}_i, [\mathbf{J}_i, \mathbf{J}_j])$, and its dimension is bigger than that of $\mathbf{J}(\mathbf{q}_0)$ provided that the $[\mathbf{J}_i, \mathbf{J}_j] \notin \text{im } \mathbf{J}$ are not filtered out by multiplication with x_i . The latter is avoided by using \mathbf{x} transversal to singular motions, as determined above. This argument is repeated for the second differential, which involves nested Lie brackets, and so on for higher-order. It was shown that this bracketing process terminates at a certain order with the smallest Lie algebra containing $\text{im } \mathbf{J}$ for all $\mathbf{q} \in \mathbb{V}^n$ [8], and this order is sufficient to generate a regular Jacobian. Thus, accordingly truncating the series expansion in terms of \mathbf{x} transversal to singular motions through \mathbf{q}_0 yields a regularizing prolongation.

6 Example: Redundant 7R Kuka LBR iiwa 14 R820

The redundant 7 DOF Kuka iiwa robot serves as a realistic example. In the reference configuration $\mathbf{q}_0 \in \mathbb{V}^7$, shown in Fig. 1b), the joint screw coordinates $\mathbf{J}_i(\mathbf{q}_0)$, deduced from the shown EE-frame, give rise to the Jacobian

$$\mathbf{J}(\mathbf{q}_0) = (\mathbf{J}_1, \dots, \mathbf{J}_7) = \begin{pmatrix} 0 & 1 & 0 & 1 & 0 & 1 & 0 \\ 0 & 0 & 0 & 0 & 0 & 0 & 0 \\ 1 & 0 & 1 & 0 & 1 & 0 & 1 \\ 0 & 0 & 0 & 0 & 0 & 0 & 0 \\ 0 & -a-b-c & 0 & -b-c & 0 & -c & 0 \\ 0 & 0 & 0 & 0 & 0 & 0 & 0 \end{pmatrix}. \quad (5)$$

The configuration is obviously singular since $\text{rank } \mathbf{J}(\mathbf{q}_0) = 3$ while the maximal rank in regular is $m = 6$. It was shown in [6] that the tangent cone to the singular motions through \mathbf{q}_0 is $C_{\mathbf{q}_0}^K L_6 = K_{\mathbf{q}_0}^{6(1)} \cup K_{\mathbf{q}_0}^{6(2)}$, with $K_{\mathbf{q}_0}^{6(1)} = \{\mathbf{x} \in \mathbb{R}^7 | x_4 = 0\}$ and

$K_{\mathbf{q}_0}^{6(2)} = \{\mathbf{x} \in \mathbb{R}^7 | x_2 = 0, x_6 = 0\}$. That is, $\text{rank} \mathbf{J} < 6$ as long as either joint 4 remains fixed or joints 2 and 6 remain locked. Thus at \mathbf{q}_0 a 6-dim and a 5-dim variety of singularities intersect, with respective tangent spaces $K_{\mathbf{q}_0}^{6(1)}$ and $K_{\mathbf{q}_0}^{6(2)}$. The detailed analysis [6] shows that this variety of singularities stratifies in to a 3-dim manifold of rank 4, a 2-dim manifold of rank 3 singularities. This is not important for solving the inverse kinematics which only needs to ensure transversality to the singular variety. The $\bar{s} = 4$ independent vectors in $K_{\mathbf{q}_0}^{6(1)} \cap K_{\mathbf{q}_0}^{6(2)}$ are

$$\begin{aligned} \mathbf{s}_1 &= (1, 0, 0, 0, 0, 0, 0)^T, \mathbf{s}_2 = (0, 0, 1, 0, 0, 0, 0)^T \\ \mathbf{s}_3 &= (0, 0, 0, 0, 1, 0, 0)^T, \mathbf{s}_4 = (0, 0, 0, 0, 0, 0, 1)^T. \end{aligned} \quad (6)$$

The projector \mathbf{N} , and the vector $\boldsymbol{\varepsilon} = (\varepsilon_1, \dots, \varepsilon_7)$ yield the vector of regularizing joint perturbations $\mathbf{x} = \mathbf{N}\boldsymbol{\varepsilon} = (0, \varepsilon_2, 0, \varepsilon_4, 0, \varepsilon_6, 0)^T$. In this singular configuration, first-order Lie brackets are sufficient to generate the closure algebra from the above joint screws: $se(3) = \text{span}(\mathbf{J}_i, [\mathbf{J}_i, \mathbf{J}_j])$. The first-order prolonged Jacobian is thus $\mathbf{J}(\mathbf{q}_0 + \mathbf{x}) = \mathbf{J}(\mathbf{q}_0) + d\mathbf{J}(\mathbf{q}_0, \mathbf{x})$, with

$$d\mathbf{J}(\mathbf{q}_0, \mathbf{x}) = \begin{pmatrix} 0 & 0 & 0 & 0 & 0 & 0 \\ 0 & -\varepsilon_2 & 0 & -\varepsilon_{24} & 0 & -\varepsilon_{246} \\ 0 & 0 & 0 & 0 & 0 & 0 \\ 0 & -\varepsilon_2(a+b+c) & 0 & -a\varepsilon_2 - (b+c)\varepsilon_{24} & 0 & -a\varepsilon_2 - b\varepsilon_{24} - c\varepsilon_{246} \\ 0 & 0 & 0 & 0 & 0 & 0 \\ 0 & 0 & a\varepsilon_2 & 0 & a\varepsilon_2 + b\varepsilon_{24} & 0 \end{pmatrix} \quad (7)$$

where $\varepsilon_{24} := \varepsilon_2 + \varepsilon_4$, $\varepsilon_{246} = \varepsilon_2 + \varepsilon_4 + \varepsilon_6$. Numerical results are computed with the geometric data $a = 0.42, b = 0.4, c = 0.126$ (all in m, units omitted) for the parameters indicated in Fig. 1b), according to the manufacturer data sheet. The desired EE-pose is expressed relative to the EE-frame in the reference configuration. The EE-pose is denoted as $\mathbf{C} = (\mathbf{R}, \mathbf{r})$ with rotation matrix \mathbf{R} and position vector \mathbf{r} .

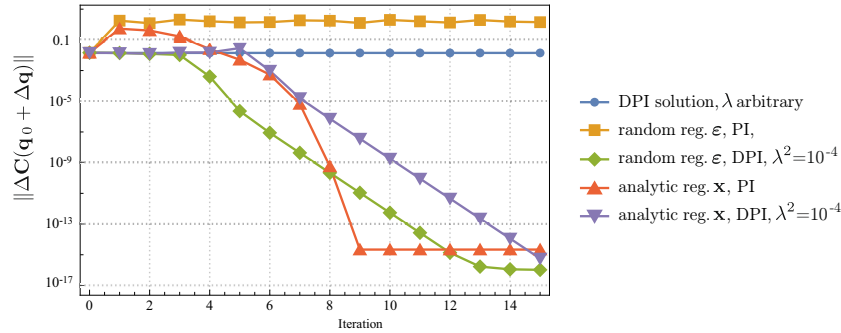


Fig. 2 Convergence for 15 iterations. Notice that the error of the DPI solution stays constant. The PI and DPI solution starting with the analytically regularized configuration as well as the DPI starting with the random perturbation converge.

1) As first example, the extreme situation is considered when the EE has to move in the x - z -plane, starting from the singular configuration, according to $\mathbf{R} = \mathbf{I}$ and $\mathbf{r} = (0.01, 0, -0.01)^T$ m. As $\Delta \mathbf{C}^V = (0, 0, 0, 0.01, 0, -0.01)^T \in \ker \mathbf{J}^T(\mathbf{q}_0) = \ker \mathbf{J}_\lambda^+(\mathbf{q}_0)$, the DPI solution (4) yields $\Delta \mathbf{q} = \mathbf{0}$, and the DLS method cannot solve the IK problem. Moreover, since columns 2, 4, and 6 of $\mathbf{J}_\lambda^+(\mathbf{q}_0)$ are zero, any instantaneous EE motion only involving translations along the y and z axis, or a rotation about the x -axis is completely annihilated.

The AI-IK method is applied with $\mathbf{x} = (0, \varepsilon_2, 0, \varepsilon_4, 0, \varepsilon_6, 0)^T$ derived above using $\varepsilon_2 = \varepsilon_4 = \varepsilon_6 = 10^{-3}$. This perturbation leads to an initial error $\|\Delta \mathbf{C}(\mathbf{q}_0 + \mathbf{x})\| \doteq 0.0145$. Since the robot is redundant, the (undamped) right PI $\mathbf{J}_{\lambda=0}^+$ is used. The convergence of the solution is shown in Fig. 2 for 15 iterations. Also shown is the result when using the DPI with $\lambda^2 = 10^{-4}$.

For comparison, the IK is solved for 20 random perturbation vectors $\boldsymbol{\varepsilon}$, with $0 \leq \varepsilon_i \leq 10^{-3}$, using Mathematica (`RandomReal[0.001, 7]`). The random numbers can be reproduced by setting the seed value of the number generator to 12345 (`SeedRandom[12345]`). The convergence of the inverse kinematics solution is shown in Fig. 2 when using the first seven random numbers as elements of $\boldsymbol{\varepsilon}$. The DPI solution converges while the undamped PI solution does not converge. To analyze the performance of the IK solution with randomly perturbed initial configuration, Fig. 3 shows the DPI solutions for all 20 random vectors $\boldsymbol{\varepsilon}$. For damping $\lambda^2 = 10^{-4}$ the solution converges for all 20 random vectors. A speed-up of the slow convergence is achieved with a smaller damping. This is shown in 3b) for $\lambda^2 = 10^{-6}$. However, the results show that this may not be sufficient to cope with the ill-conditioned, and possibly singular, Jacobian obtained with random perturbations.

2) The EE is now following a general motion. The target EE pose at the sampling step after the singularity is computed as $\mathbf{C}_d = f(\mathbf{q}_0 + \Delta \mathbf{q}_d)$, with $\Delta \mathbf{q}_d = (0.01, 0.01, 0.05, 0.01, 0.01, 0.01, 0.05)^T$. The convergence of the iteration methods are shown in Fig. 4. The DPI method yields a numerical solution, and exhibits the known convergence property for $\lambda^2 = 10^{-4}$. The iteration starting with the analyt-

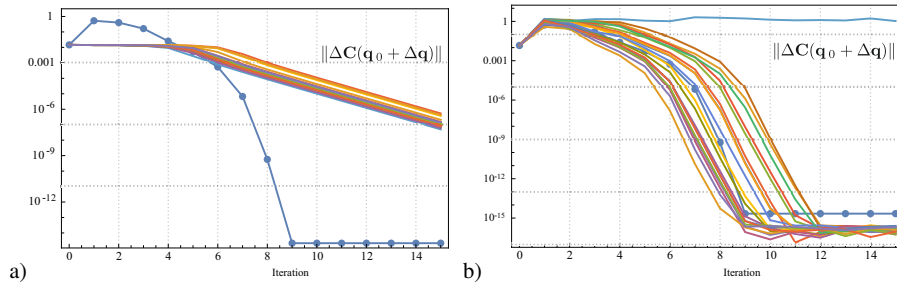


Fig. 3 Convergence of the DPI for 20 different random perturbations (curves without markers), when a) $\lambda^2 = 10^{-4}$ and b) $\lambda^2 = 10^{-6}$. For comparison, the PI solution obtained with the analytically regularized start configuration is included.

ically regularized Jacobian and with the randomly perturbed Jacobian (\mathbf{x} and $\boldsymbol{\varepsilon}$ as above) show similar convergence rates when using the DPI. The undamped PI solutions achieve the most accurate solutions. The convergence of the DPI solution, when starting from the perturbed configurations according to the 20 different random vectors $\boldsymbol{\varepsilon}$, is shown in Fig. 5. Additionally, results of the DPI solution and the PI solution with perturbation \mathbf{x} (AI-IK solution) are shown again.

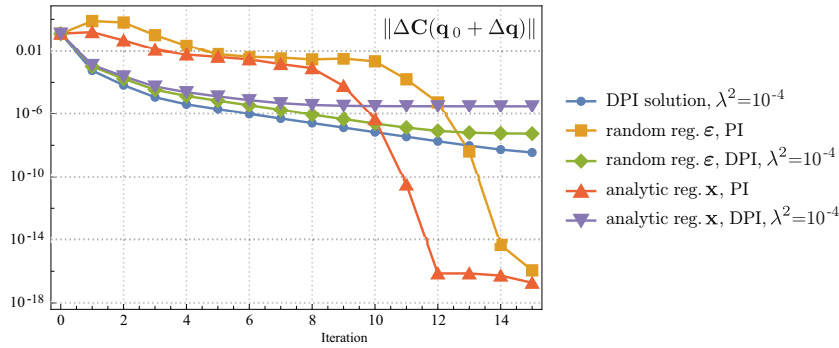


Fig. 4 Convergence during 15 iterations when perform a general motion starting at the singularity.

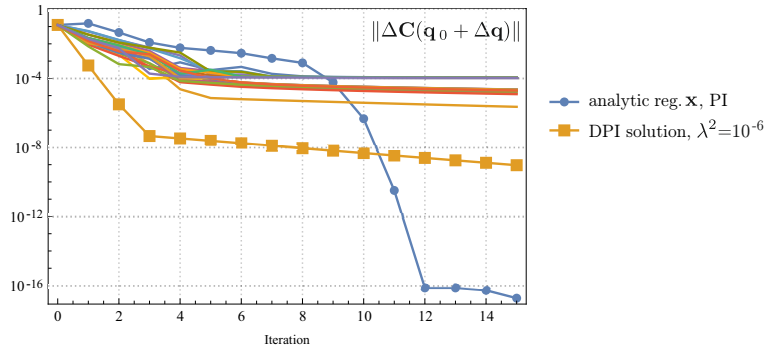


Fig. 5 Convergence of the DPI for 20 different random perurbations (curves without markers), when $\lambda^2 = 10^{-6}$. For comparison, the PI solution obtained with the analytically regularized start configuration, and the DPI solution with $\lambda^2 = 10^{-6}$ are included.

From the examples it may be concluded that at singularities, the AI-IK method should be used. This ensures that a solution of the IK problem will always be found as this method is robust against the 'lock-up' phenomenon observed in the first test situation. To further increase robustness, the DPI of the regularized Jacobian may be used.

7 Conclusion

A lesser known problem of singular configurations of robotic manipulators is that any PI-based IK solution method fails when instantaneous EE motions necessary to reach a desired configuration is not feasible, i.e. the desired EE-velocities are in the null-space of \mathbf{J}^T . To overcome this problem, a solution method was proposed that is robust against such situations. It relies on a perturbation away from the singularity, which is obtained from a local analysis of the singular motions using the kinematic tangent cone. The latter can be determined offline since the singularities of the robot should be known. The method was shown for the classical stretched arm singularities, but is applicable to general singularities. Future work will address an informed choice of perturbation magnitude. Another aspect to be addressed is how a preference for certain inverse kinematics solution branches can be taken into account.

Acknowledgements This work was supported by the LCM-K2 Center within the framework of the Austrian COMET-K2 program, and by the Austrian Science Fund (FWF) [I 4452-N]

References

1. Chan, S.K., Lawrence, P.D.: General inverse kinematics with the error damped pseudoinverse. In: Proceedings. 1988 IEEE Int. Conf. on Robotics and Automation, pp. 834–839 (1988)
2. Chiaverini, S.: Singularity-robust task-priority redundancy resolution for real-time kinematic control of robot manipulators. *IEEE Trans. on Robotics and Automation* **13**(3), 398–410 (1997)
3. Deo, A.S., Walker, I.D.: Adaptive non-linear least squares for inverse kinematics. In: Proceedings IEEE International Conference on Robotics and Automation, pp. 186–193 (1993)
4. Husty, M.L., Pfurner, M., Schröcker, H.P.: A new and efficient algorithm for the inverse kinematics of a general serial 6r manipulator. *Mechanism and machine theory* **42**(1), 66–81 (2007)
5. Mayorga, R.V., Wong, A.K., Milano, N.: A fast procedure for manipulator inverse kinematics evaluation and pseudoinverse robustness. *IEEE Transactions on Systems, Man, and cybernetics* **22**(4), 790–798 (1992)
6. Müller, A.: Higher-order analysis of kinematic singularities of lower pair linkages and serial manipulators. *ASME J. Mech. Rob.* **10**(1) (2018)
7. Müller, A.: Local investigation of mobility and singularities of linkages. In: A. Müller, D. Zlatanov (eds.) *Singular Configurations of Mechanisms and Manipulators*, CISM 589. Springer (2019)
8. Müller, A.: An overview of formulae for the higher-order kinematics of lower-pair chains with applications in robotics and mechanism theory. *Mech. Mach. Theory* **142** (2019)
9. Nakamura, Y., Hanafusa, H.: Inverse kinematic solutions with singularity robustness for robot manipulator control. *ASME J. Dyn. Sys., Meas., Control.* **108**(3), 163–171 (1986)
10. Raghavan, M., Roth, B.: Inverse kinematics of the general 6r manipulator and related linkages **115**(3), 502–508 (1993)
11. Siciliano, B.: A closed-loop inverse kinematic scheme for on-line joint-based robot control. *Robotica* **8**(3), 231–243 (1990)
12. Wampler, C.W.: Manipulator inverse kinematic solutions based on vector formulations and damped least-squares methods. *IEEE Tran. Systems, Man, and Cybernetics* **16**(1), 93–101 (1986)